Proc. Natl. Acad. Sci. USA
Vol. 93, pp. 15429–15434, December 1996
Neurobiology

A regenerative link in the ionic fluxes through the *weaver* potassium channel underlies the pathophysiology of the mutation

SCOTT K. SILVERMAN*, PAULO KOFUJI†, DENNIS A. DOUGHERTY*, NORMAN DAVIDSON†, AND HENRY A. LESTER†‡

Divisions of *Chemistry and Chemical Engineering and †Biology, California Institute of Technology, Pasadena, CA 91125

Contributed by Norman Davidson, October 16, 1996

ABSTRACT **The homozygous *weaver* mouse displays neuronal degeneration in several brain regions. Previous experiments in heterologous expression systems showed that the G protein-gated inward rectifier K^+ channel (GIRK2) bearing the *weaver* pore-region GYG-to-SYG mutation (i) is not activated by $G_{\beta\gamma}$ subunits, but instead shows constitutive activation, and (ii) is no longer a K^+-selective channel but conducts Na^+ as well. The present experiments on *weaver*GIRK2 (*wv*-GIRK2) expressed in *Xenopus* oocytes show that the level of constitutive activation depends on intracellular Na^+ concentration. In particular, manipulations that decrease intracellular Na^+ produce a component of Na^+-permeable current activated via a G protein pathway. Therefore, constitutive activation may not arise because the *weaver* mutation directly alters the gating transitions of the channel protein. Instead, there may be a regenerative cycle of Na^+ influx through the *wv*GIRK2 channel, leading to additional Na^+ activation. We also show that the *wv*GIRK2 channel is permeable to Ca^{2+}, providing an additional mechanism for the degeneration that characterizes the *weaver* phenotype. We further demonstrate that the GIRK4 channel bearing the analogous *weaver* mutation has properties similar to those of the *wv*GIRK2 channel, providing a glimpse of the selective pressures that have maintained the GYG sequence in nearly all known K^+ channels.**

The *weaver* mouse carries the first vertebrate ion channel mutation associated with a developmental defect. The single-nucleotide mutation changes a glycine residue to serine in the pore region of the G protein-gated inward rectifier K^+ channel (GIRK2), altering the highly conserved and critical GYG sequence to SYG (1). In homozygotic *weaver* mice, the mutation causes degeneration of the cerebellar granule cells during migration from the external germinal layer to the granule cell layer (2–4), degeneration of the *substantia* nigra pars compacta (5), cytoarchitectonic anomalies in the CA3 region of the hippocampus (6), seizures, and male sterility.

How does the *weaver* mutation cause these defects? Previous studies showed that the *weaver*GIRK2 (*wv*GIRK2) channel expressed in heterologous systems displays three new functional properties: (*i*) *wv*GIRK2 no longer requires activation by $G_{\beta\gamma}$ subunits, but instead shows constitutive activation; (*ii*) *wv*GIRK2 is no longer selective for K^+, but conducts Na^+ as well; and (*iii*) *wv*GIRK2 is sensitive to blockade by several drugs, including QX-314, MK-801, and verapamil, that block other cation channels (7–10). In a previous study (8), this drug sensitivity was exploited: when *weaver* granule cells were incubated in culture with cation channel blockers, they survived, extended neurites, and displayed a marker of differentiation. The degenerative *weaver* phenotype is explained by the straightforward hypothesis that Na^+ influx through the mutant channel eventually overloads the Na^+ extrusion capabilities of the granule cell, leading to collapse of the Na^+ gradient, the resulting collapse of other gradients driven directly or indirectly by Na^+, and eventual cell death.

However, several uncertainties remain. It is not known whether the constitutive activation is inherent to the mutant *wv*GIRK2 channel protein or is an indirect consequence of other properties. Furthermore, there are important and unexplained differences among the results of recent studies. The constitutive activation is incomplete in oocytes injected with small quantities of *wv*GIRK2 mRNA (7). In excised patches, openings of *wv*GIRK2 channels are sparse, inconsistent with the hypothesis of constitutive activation (9). Although one study found the expected standing Na^+ currents in *weaver* granule cells (8), another did not (11). Although two laboratories found G protein-gated K^+ currents in normal but not *weaver* granule cells (8, 11), another found no such currents in normal or *weaver* cells (12). These variable results suggest that some important factor has not yet been systematically controlled.

Intracellular Na^+ is a good candidate for this uncontrolled factor, because wild-type GIRK1/GIRK2 heteromultimeric channels (13) as well as wild-type GIRK1/GIRK4 heteromultimeric channels (14) are activated in a $G_{\beta\gamma}$-independent fashion by intracellular Na^+ in the mM concentration range. We present new data suggesting that the $G_{\beta\gamma}$-independent activation of *wv*GIRK2 channels arises as a consequence of activation by intracellular Na^+. We also find that *wv*GIRK2 channels are permeable to Ca^{2+}, unlike channels containing wild-type GIRK2, providing another general mechanism for cellular degeneration in the *weaver* mouse (15). We have further asked whether the GYG-to-SYG mutation causes the *weaver* phenotype in other GIRK channels, and we find that *wv*GIRK4 does display a phenotype similar to that of *wv*-GIRK2, while *wv*GIRK1 expresses poorly.

MATERIALS AND METHODS

Site-Directed Mutagenesis. A two-step PCR procedure was employed as follows: two complementary oligonucleotides incorporating the desired point mutations were synthesized and paired with appropriate outer primers in a first round of PCR using *Pfu* polymerase (Stratagene). The PCR products were purified on agarose gel, then combined with each other and the two outer primers from the first round of PCR, and a second round of PCR was performed. The second PCR product was gel-purified and trimmed on each end with an appropriate restriction enzyme. This product was gel-purified and ligated into the parent construct, which was previously digested with the same two restriction enzymes and dephosphorylated. All sequences originating in PCR were verified by automated sequencing over the entire amplified region and the ligation sites.

The publication costs of this article were defrayed in part by page charge payment. This article must therefore be hereby marked "*advertisement*" in accordance with 18 U.S.C. §1734 solely to indicate this fact.

Abbreviations: GIRK, G protein-gated inward rectifier K^+; *wv*, *weaver*; ACh, acetylcholine; NMDG, *N*-methyl-D-glucamine; m2AChR, m2 muscarinic acetylcholine receptor; XIR, oocyte inward rectifier.

‡To whom reprint requests should be addressed. e-mail: lester@caltech.edu.

DNA Clones. Rat GIRK1 (KGA), mouse GIRK2, and mouse *wv*GIRK2 were available from previous studies (8, 16). Rat GIRK4 was obtained from J. Adelman (17). The m2 muscarinic acetylcholine receptor (m2AChR) was obtained from E. Peralta (18) and was in the pGEM3Z vector. All GIRK constructs were subcloned into the pMXT vector, obtained from L. Salkoff (19). The m2AChR was linearized with *Hin*dIII, and mRNA was transcribed using the T7 polymerase mMessage mMachine kit from Ambion (Austin, TX). All GIRK constructs were linearized with *Sal*I, and mRNA was transcribed using the T3 polymerase mMessage mMachine kit. mRNA concentration was estimated by both UV absorption (A_{260}) and intensity on an ethidium bromide-stained agarose gel.

Oocyte Preparation and Injection. Oocytes were removed from *Xenopus laevis* as described (20) and maintained at 18°C in various solutions, which were changed twice daily. The standard solution (ND96) consisted of 96 mM NaCl, 2 mM KCl, 1 mM $MgCl_2$, 1.8 mM $CaCl_2$, and 5 mM Hepes supplemented with 2.5 mM sodium pyruvate, 50 mg/ml gentamicin, and 0.6 mM theophylline (pH 7.5), further supplemented in most cases with 5% horse serum. For ionic substitutions, the total monovalent cation concentration was maintained at 98 mM with *N*-methyl-D-glucamine (NMDG), and pH was adjusted with either NaOH or HCl. Oocytes were injected with 50 nl of water solution containing mRNA and, when appropriate, 12.5 ng of fully phosphothioated oocyte inward rectifier (XIR) antisense oligonucleotide KHA2 (5′-CTGAGGACTTGGTGCCATTCT-3′) (21), prepared at the Biopolymer Synthesis facility of the Beckman Institute at California Institute of Technology. Injected amounts of mRNAs were as follows: *wv*GIRK2, 5 ng; *wv*GIRK4, 25 ng; wild-type GIRK1, GIRK2, or GIRK4, 1.25 ng; and m2AChR, 3 ng.

Electrophysiology. Two-electrode voltage clamp recordings were performed 11–48 hr postinjection at room temperature (≈20°C) using a GeneClamp 500 amplifier and pCLAMP software (Axon Instruments, Foster City, CA) (20). Microelectrodes were filled with 3 M KCl and had resistances of 0.5–2 MΩ. Oocytes were continuously perfused with a bath solution of 98 mM NaCl or KCl, 1 mM $MgCl_2$, and 5 mM Hepes (pH 7.5 with NaOH/KOH); or 98 mM NMDG, 1 mM $MgCl_2$, and 5 mM Hepes (pH 7.5 with HCl) (exposure to K^+-free solutions was brief to avoid losing intracellular K^+). In some instances where large currents were observed, the Na^+ concentration was lowered to 25 mM, replacing NaCl with NMDG. Currents were quantified at −80 mV and are reported as mean ± SEM.

RESULTS

Constitutive Activation of *wv*GIRK2 Depends on Intracellular Na^+. Oocytes were injected with mRNAs coding for *wv*GIRK2 and m2AChR, then incubated for 11–30 hr in the standard solution (96 mM Na^+/2 mM K^+) and studied with a two-electrode voltage clamp circuit. When the recording chamber was perfused with a Na^+ solution, we observed inward currents of up to 5 μA in amplitude at a holding potential of −80 mV (Fig. 1*A*). In addition to this constitutively activated Na^+ current, ACh activated additional Na^+ current (up to 35% of the total current). Under comparable conditions, wild-type GIRK2 gives no significant current (8). The fraction of the current that is constitutively activated correlates well with the total Na^+ current (Fig. 1*B*), showing a monotonic increase from 65% at the lowest detectable levels (≈100 nA) to 100% at total currents above 2 μA. There is a poorer correlation between the constitutively active current and the time since injection (Fig. 1*B Inset*), and therefore we present our data in terms of total Na^+ current. As shown in greater detail below, *wv*GIRK4 also displays both constitutively activated and ACh-induced Na^+ currents with properties generally similar to those of *wv*GIRK2.

The hypothesis of intracellular Na^+ involvement prompted us to test for the role of Na^+ entry through the *wv*GIRK2 channel itself. However, incubation of *wv*GIRK2-injected oocytes in the standard medium supplemented with 100 μM QX-314 (IC_{50} for *wv*GIRK2, ≈11 μM) (8) did not alter the activation profile when currents were measured in the absence of QX-314 (Fig. 1*B*). This implies that the main route of Na^+ entry in oocytes is not through *wv*GIRK2, so we sought other means of affecting the intracellular Na^+ concentration. Ouabain is an effective blocker of Na^+,K^+-ATPase, which maintains a low intracellular Na^+ concentration in all animal cell types. When 100 μM ouabain was added to the incubation medium used for bathing *wv*GIRK2-injected oocytes, the fraction of constitutively activated current was higher at any total current level (Fig. 1*C*), as expected if the *wv*GIRK2 channel is activated by intracellular Na^+. The actual ACh-induced component of the Na^+ current never exceeded 80 nA for the oocytes incubated in ouabain; for oocytes incubated in the standard solution, the ACh-induced current was as large as 190 nA (Fig. 1*D*).

We also tested *wv*GIRK2-injected oocytes incubated in 8 mM Na^+/20 mM K^+ supplemented with 5 mM glucose (NMDG comprised the balance of the monovalent cations). This solution is expected to reduce Na^+ influx as well as enhance the pumping activity of Na^+,K^+-ATPase. When these oocytes were tested in 98 mM Na^+, the fraction of constitutively activated current was smaller for a given total current level (Fig. 1*C*). Constitutive activation was only 45% at the lowest detectable total current levels; at total current levels of 2 μA, constitutive activation was only 70–85%, in contrast to 100% for oocytes incubated in the standard solution. The actual ACh-induced component of Na^+ current, dramatically larger than for the other incubation conditions, was as high as 650 nA and continued to increase at the highest total current levels recorded (≈3 μA). Thus, a manipulation that decreases intracellular Na^+ restores some normal gating via a G protein pathway, but the channels retain their Na^+ permeability. Incubation in 78 mM Na^+/20 mM K^+ with 5 mM glucose provided an intermediate effect (data not shown).

***wv*GIRK2 Channels Are Permeable to Ca^{2+}.** Oocytes expressing *wv*GIRK2 showed large (several microamperes) responses to 5 mM extracellular Ca^{2+} (Fig. 2*A*); no similar responses were observed in uninjected oocytes or in oocytes injected with wild-type GIRK1, GIRK2, or GIRK1 + GIRK2 mRNAs. The responses to Ca^{2+} were observed even with no permeant monovalent cations present in the extracellular solution (Na^+ was replaced by impermeant NMDG; Fig. 2*A*). The Ca^{2+}-induced response was blocked by 300 μM QX-314 yet appeared within a few seconds after QX-314 was washed from the chamber (Fig. 2*A*). This rapid time course and the independence on extracellular Na^+ both argue against Ca^{2+} entry via indirect pathways mediated by possible changes in the Na^+ gradient. Thus, Ca^{2+} permeates the *wv*GIRK2 channel through the pathway blocked by QX-314. Similar results were obtained for *wv*GIRK4 (Fig. 2*B*), as described in detail below.

The several-microampere currents induced by 5 mM Ca^{2+} are larger than any known direct Ca^{2+} currents and are arguably too large in any case to be carried directly by Ca^{2+}. However, signals this large are expected from Ca^{2+}-activated Cl^- channels (22). The even larger, transient (<5 s) components of inward current upon application of Ca^{2+} are also expected, as shown in previous studies (23). To verify the role of Ca^{2+}-activated Cl^- channels, we replaced most of the extracellular Cl^- with methanesulfonate and determined the shift in reversal potential (ΔE_{rev}). With 5 mM Ca^{2+} as the only permeant extracellular cation, the ΔE_{rev} on decreasing the extracellular [Cl^-] from 110 to 10 mM for *wv*GIRK2 was +33.9 ± 0.4 mV (n = 4), which is a large fraction of the +58

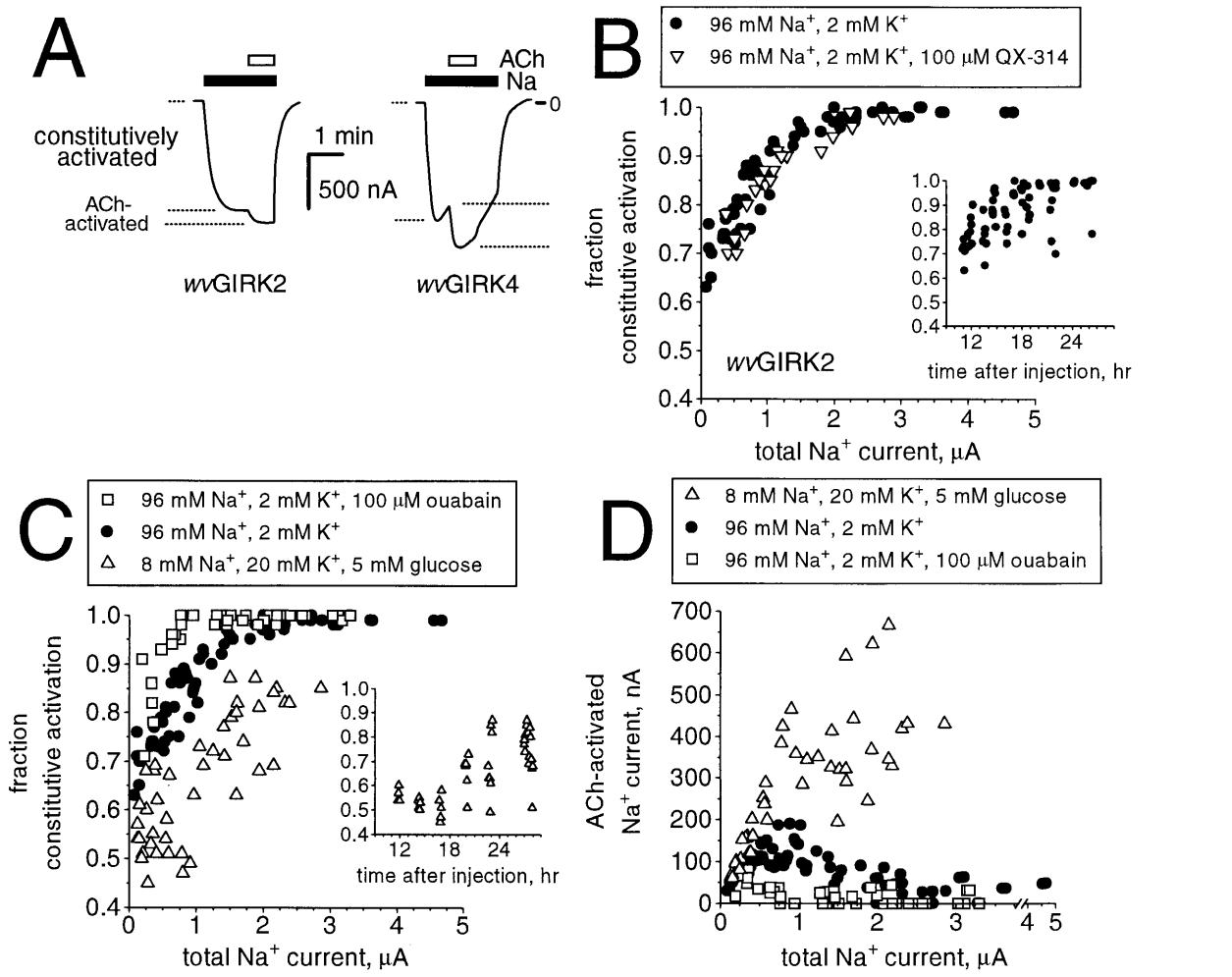

FIG. 1. Constitutive activation of *wv*GIRK2 and *wv*GIRK4 is increased by intracellular Na^+. (*A*) Representative traces from oocytes injected with 3 ng m2AChR mRNA plus either 5 ng *wv*GIRK2 mRNA or 25 ng *wv*GIRK4 mRNA, held at a membrane potential of −80 mV. The traces show the constitutively activated Na^+ current and the acetylcholine (ACh)-activated Na^+ current. Bars indicate application of 98 mM Na^+ and 1 μM ACh; where no bar is shown, the bath solution contained 98 mM NMDG as the only monovalent cation. (*B*) Variation of constitutive activation with total Na^+ current for *wv*GIRK2-injected oocytes incubated in the standard medium (96 mM Na^+/2 mM K^+) with (●) or without (▽) 100 μM QX-314, but tested in the absence of QX-314. Each data point represents a single oocyte from either three or two separate batches, respectively. (*Inset*) Variation of constitutive activation with time since injection. (*C*) Variation of constitutive activation with total Na^+ current for *wv*GIRK2-injected oocytes incubated in the standard medium alone (●), standard medium with 100 μM ouabain (□), or 8 mM Na^+, 20 mM K^+ with 5 mM glucose (△). Each data point represents a single oocyte from either two, three, or one separate batch(es), respectively. (*Inset*) Variation of constitutive activation with time since injection. (*D*) The data of *C* are presented as ACh-induced currents for the three experimental manipulations.

mV expected for a pure Cl^- conductance (data not shown). Experiments with Na^+ included in the extracellular medium produced similar results.

Voltage-jump experiments provide further evidence both for the permeability of Ca^{2+} through the *wv*GIRK2 channel and for the identification of Cl^- as the ion responsible for the Ca^{2+}-induced currents. Upon bath application of 5 mM Ca^{2+}, the directions and time courses of voltage-jump currents are very similar to those observed when Ca^{2+} is released into the cytoplasm via other mechanisms, such as InsP_3 injection (24), phospholipase C activation, A23187 application (23), or activation of voltage-gated Ca channels (25, 26) (Fig. 2*C*). The E_{rev} for these currents was -25.7 ± 0.3 mV ($n = 8$), as expected for a Cl^- conductance (22).

The *wv*GIRK4 Channel Functions Similarly to *wv*GIRK2. The GYG sequence is also found in the pore region of GIRK4. We constructed the SYG mutant of GIRK4, which we term *wv*GIRK4. Expressed in oocytes, *wv*GIRK4 channels are permeable to both Na^+ and K^+ (Fig. 3*A*), with a permeability ratio $P_{Na}/P_K = 0.90 \pm 0.04$ from reversal potential measurements like those of Fig. 3*B*. Thus, *wv*GIRK4 has an even higher P_{Na}/P_K ratio than the value of 0.5 determined for *wv*GIRK2 (8). Like *wv*GIRK2, *wv*GIRK4 displays much diminished inward rectification compared with the wild-type channel (Fig. 3*B*). Large currents in 98 mM extracellular Rb^+ and Cs^+ were also observed (data not shown), as they are for *wv*GIRK2. An intriguing difference between *wv*GIRK2 and *wv*GIRK4 is in the desensitization of the currents during exposure to Na^+ or K^+ (Fig. 3*A*). *wv*GIRK2 exhibits very little desensitization with either ion. In contrast, *wv*GIRK4 shows slow desensitization upon application of Na^+ (<10% in 1 min, similar to that of wild-type GIRK heteromultimers with K^+), but rather rapid desensitization upon exposure to K^+ (≈50% in 1 min).

As observed for the *wv*GIRK2 channel, the constitutive activation of *wv*GIRK4 correlates with the magnitude of total current (Fig. 3*C*), although the level of constitutive activation is somewhat lower for *wv*GIRK4. Also as for the *wv*GIRK2 channel, *wv*GIRK4 is permeable to Ca^{2+} (Fig. 2*B*). For *wv*GIRK4, the Ca^{2+} response is largely blocked by 300 μM QX-314. Moreover, the response is ≈50% blocked by 50 μM QX-314, which is near the IC_{50} (see below). Voltage-jump experiments on *wv*GIRK4 similar to those of Fig. 2*C* (not

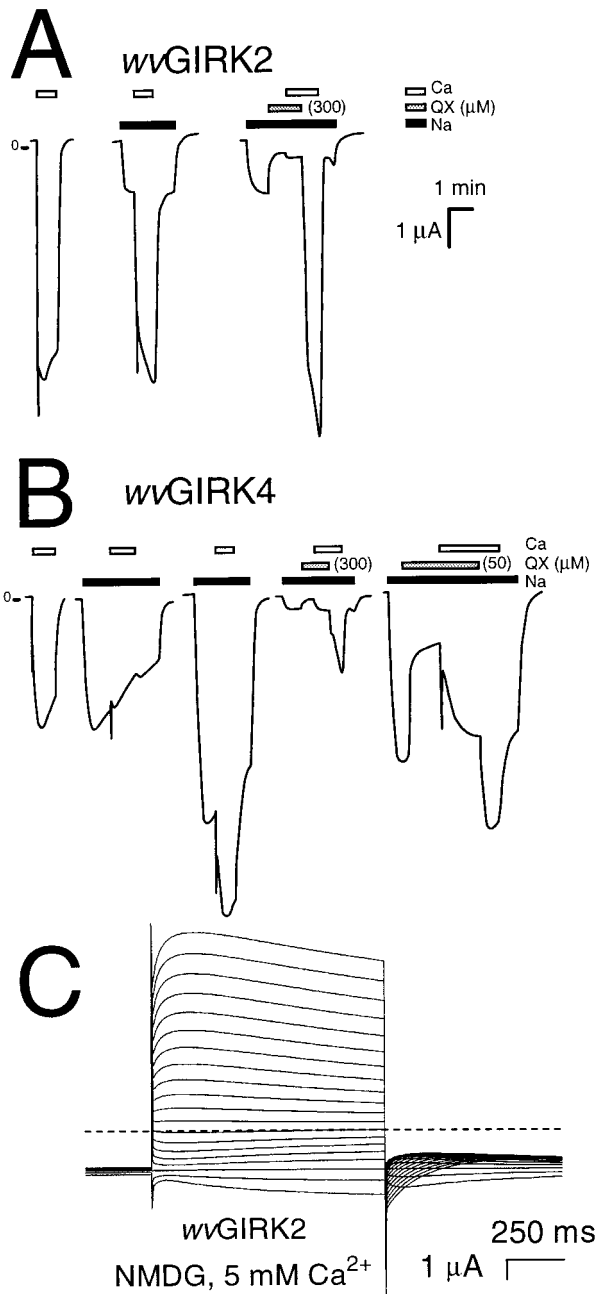

FIG. 2. *wv*GIRK2 and *wv*GIRK4 channels are permeable to Ca^{2+}. (*A*) Representative traces from oocytes injected with 5 ng *wv*GIRK2 mRNA. Bars indicate application of 98 mM Na^+; 300 μM QX-314; and 5 mM Ca^{2+}. In the third trace, 25 mM Na^+ was used. Where no bar is shown, the bath solution contained 98 mM NMDG as the only monovalent cation. The large, transient (<5 s) inward currents upon application of Ca^{2+} are highly reproducible and are not artifacts, since they are observed only with Ca^{2+}. Note that the Ca^{2+}-induced currents are suppressed by QX-314. (*B*) Traces from oocytes injected with 25 ng *wv*GIRK4 mRNA. Bars indicate application of 98 mM Na^+; 300 or 50 μM QX-314 as shown; and 5 mM Ca^{2+}. In the fourth trace, 25 mM Na^+ was used. (*C*) Representative voltage-jump records from an oocyte injected with 5 ng *wv*GIRK2 mRNA and exposed to 5 mM Ca^{2+} in 98 mM NMDG solution. The membrane potential was held at -80 mV then stepped to test potentials between -100 and $+90$ mV in 10 mV increments for 1 s, at intervals of 5 s. The dashed line indicates zero current. No subtractions were performed, and currents were not corrected for desensitization.

shown) demonstrate that Cl^- is the conducting ion (E_{rev}, -29.1 ± 1.7 mV, $n = 7$).

To address the issue of possible coassembly with the endogenous oocyte inward rectifier subunit XIR/GIRK5 (21), *wv*GIRK4 was coinjected with an antisense oligonucleotide (KHA2) directed against XIR. For *wv*GIRK4 alone, the Na^+ currents were 3.1 ± 0.5 μA ($n = 8$), and for *wv*GIRK4 plus KHA2 the signals were 3.0 ± 0.5 μA ($n = 9$). Other experiments showed that our sample of KHA2 can effectively suppress XIR (27). Therefore, when currents are large, at most a minor portion of the *wv*GIRK4 signal is due to coassembly with XIR.

We also constructed the *weaver* mutation, GYG to SYG, in the GIRK1 channel. In contrast to *wv*GIRK2 and *wv*GIRK4, *wv*GIRK1 showed little functional expression in oocytes. In three experiments, Na^+ currents from *wv*GIRK4 were 4–8 μA, while those from *wv*GIRK1 averaged 16 ± 2 nA ($n = 5$), 276 ± 25 nA ($n = 5$), and 740 ± 47 nA ($n = 6$). The small signals from *wv*GIRK1 are probably due to homomultimers, not to coassembly with endogenous XIR, since wild-type GIRK4 (highly homologous to XIR) did not enhance the signals from *wv*GIRK1 alone (data not shown). Coexpression of *wv*GIRK1 with *wv*GIRK4 significantly suppressed the signal from *wv*GIRK4 alone, although the magnitude of the decrease was variable (in four experiments, the suppressions averaged 98, 70, 56, and 37%). In contrast, coexpression of either wild-type GIRK1 or GIRK4 with *wv*GIRK4 did not affect the signal from *wv*GIRK4 alone (data not shown).

We determined IC_{50} for the channel blocker QX-314 for a number of subunit combinations. Wild-type GIRK channels are insensitive to QX-314, but the *weaver* mutation confers sensitivity (Fig. 3*A*). *wv*GIRK2 has an IC_{50} of ≈ 11 μM when expressed under similar conditions (8). For *wv*GIRK4, we found a higher IC_{50}: two determinations in separate oocyte batches gave 51 ± 3 μM and 60 ± 8 μM (Fig. 3*D*). When *wv*GIRK4 was coexpressed with wild-type GIRK4, the IC_{50} was not detectably different (59 ± 9 μM), but there was perhaps a slight drop when *wv*GIRK4 was coexpressed with wild-type GIRK1 (36 ± 4 μM). The currents from *wv*GIRK1 plus *wv*GIRK4 (IC_{50}, 18 ± 2 μM) were threefold more sensitive to QX-314 than those from *wv*GIRK4 alone (data not shown). Like the *wv*GIRK2 channel (8), the *wv*GIRK4 channel is also substantially blocked by 50 μM MK-801 (Fig. 3*A*).

DISCUSSION

Experimental manipulation of intracellular Na^+ (Fig. 1) reveals that two characteristics of the *wv*GIRK2 channel, Na^+ permeability and constitutive activation, can be separated. In particular, the level of constitutive activation is increased or decreased by incubations that increase or decrease the intracellular Na^+ concentration (Fig. 1*C*). Thus, constitutive activation may not arise because the *weaver* mutation has directly increased the fraction of activation that is independent of G protein activation, but could instead be a secondary consequence of intracellular Na^+ accumulation. Under conditions leading to low intracellular Na^+, robust (several hundred nanoamperes) Na^+-permeable responses can be elicited via the G protein-activated pathway (Fig. 1*D*).

The activation by intracellular Na^+ is expected from experiments on channels containing wild-type GIRK2 and GIRK4 subunits (13, 14). For these wild-type channels, the Na^+-dependent activation may have a physiological benefit, helping to hyperpolarize the cell (14). For the Na^+-permeable *wv*GIRK2 channel, however, the Na^+ influx would enhance the channel activity and lead to a disastrous further influx of Na^+. This regenerative process would be swiftest in cells with a high surface-to-volume ratio, such as granule cells. A cerebellar granule cell is the smallest neuron in the vertebrate central nervous system, and its diameter is 100-fold lower than that of a *Xenopus* oocyte. A major difference that we observed between the oocyte and the granule cell was the lack of protective effects of QX-314 in the oocyte experiments (Fig. 1*B*), although this and other channel-blocking drugs were able

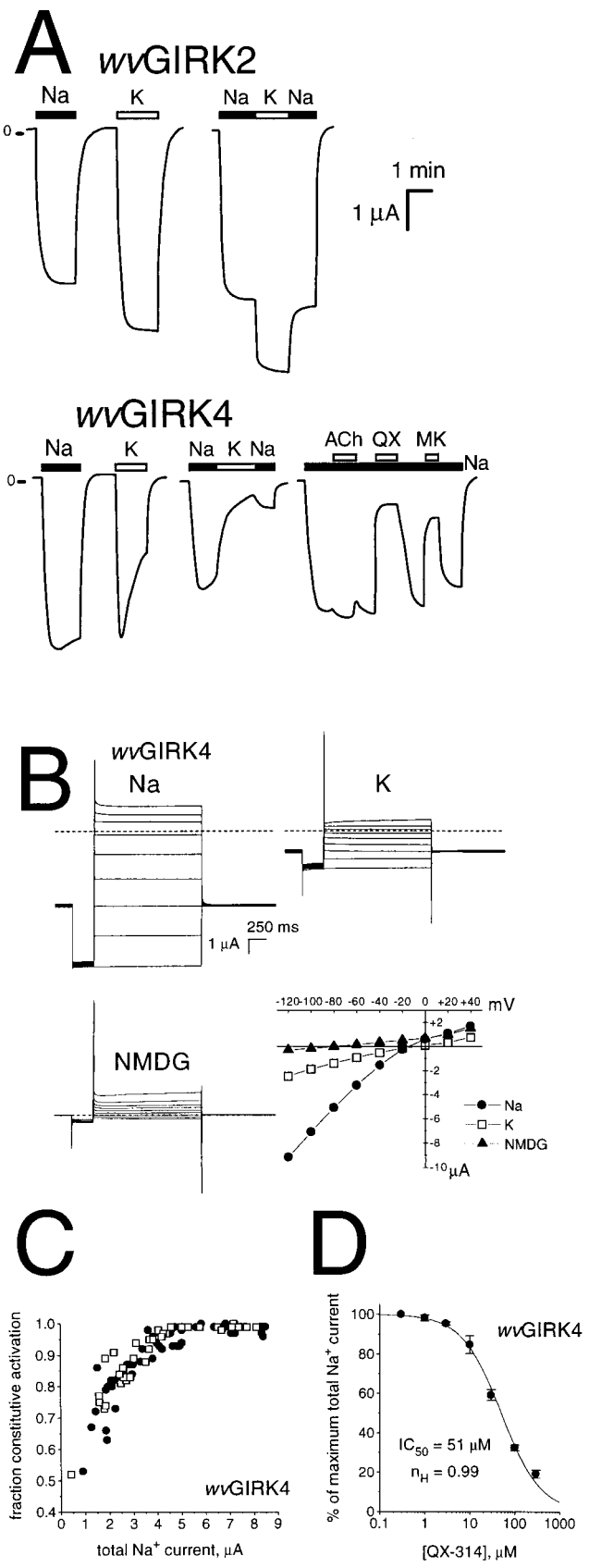

FIG. 3. The *wv*GIRK4 channel functions similarly to *wv*GIRK2. (*A Upper*) Representative traces from oocytes injected with 5 ng *wv*GIRK2 mRNA and 3 ng m2AChR mRNA. Bars indicate application of 98 mM Na^+ or K^+. (*A Lower*) Representative traces from oocytes injected with 25 ng *wv*GIRK4 mRNA and 3 ng m2AChR mRNA. Bars indicate application of 98 mM Na^+ or K^+, 1 μM ACh, 100 μM QX-314, or 50 μM MK-801. Where no bar is shown, the bath solution contained 98 mM NMDG as the only monovalent cation. (*B*) Representative voltage-jump records from an oocyte injected with 25 ng *wv*GIRK4 mRNA. The membrane potential was held at −80 mV, stepped to −120 mV for 300 ms, then stepped to test potentials between −120 and +40 mV in 20-mV increments for 1500 ms, at intervals of 7 s. The dashed lines indicate zero current. No subtractions were performed, and currents were not corrected for desensitization. The extracellular solution contained 98 mM Na^+, K^+, or NMDG as the only monovalent cation. The plot shows current-voltage relations for the voltage-step records, with points taken from immediately before the step back to −80 mV. (*C*) Variation of constitutive activation with total Na^+ current for *wv*GIRK4-injected oocytes incubated in the standard medium. ●, *wv*GIRK4 mRNA alone; □, *wv*GIRK4 plus either *wv*GIRK1, GIRK1, or GIRK4. (*D*) Dose-response relation for QX-314 blockade of *wv*GIRK4 Na^+ currents.

to rescue *weaver* granule cells in culture (8). Thus, although the constitutive activation of *wv*GIRK2 depends on intracellular Na^+, in oocytes the primary source of this Na^+ is not entry through the *wv*GIRK2 channel itself, whereas in granule cells this is apparently the case. It seems likely that the oocyte expresses many Na^+-dependent transporters that account for most of the Na^+ influx.

That QX-314 does not affect constitutive activation raises questions about an additional feature of the data: the level of constitutive activation rises with total current (Fig. 1*B*). One possible explanation is that all of the functional channels are *wv*GIRK2 homomultimers, whose constitutive activation changes with total expression via an unknown mechanism. A second explanation asserts that there are several functional channel types, all of which are Na^+ permeable, but some of which incorporate subunits other than *wv*GIRK2. In oocytes, a candidate for another contributing subunit is the endogenous XIR (GIRK5). If *wv*GIRK2/XIR heteromultimers are less Na^+ sensitive than homomultimeric *wv*GIRK2 channels, the effect of XIR would be most pronounced at low total expression levels, where it is relatively likely for a multimer to incorporate an endogenous subunit, and this would account for the curvature in Fig. 1*B*. For measurements made shortly after injection, the incorporated XIR is present initially in the oocyte, and antisense suppression of XIR should have little effect. At high expression levels, most multimers would comprise only *wv*GIRK2 subunits, and XIR (or antisense suppression thereof) would be unimportant, as observed. In general, it will be important to understand whether other GIRK subunits (e.g., GIRK1) interact with *wv*GIRK2 in neurons, as appears to be the case in heterologous expression systems (7–9).

We note that not all cells expressing GIRK2 degenerate simultaneously in the *weaver* mouse; some fail to degenerate at all (7, 8, 28). These differences are probably caused by several factors, including the detailed time course of GIRK2 expression, expression of other GIRK channels, size of the cell, presence of pumps and transporters in the cell membrane, and other metabolic demands on the cell.

Our conclusion that Ca^{2+} flows through the *wv*GIRK2 and *wv*GIRK4 channels (Fig. 2) is based on the Ca^{2+}-activated Cl^- conductance, which provides a more sensitive detector system for Ca^{2+} influx than does direct current measurements (25, 26). We detect no Ca^{2+} permeability in wild-type GIRK2 or GIRK1/GIRK2 channels expressed in oocytes. The view of *wv*GIRK2 as a nonspecific cation channel must therefore be broadened to include the divalent Ca^{2+} ion as well. At present we cannot estimate the ratio of Ca^{2+} to Na^+ conductances for *wv*GIRK2 and *wv*GIRK4, but it must be rather small because Navarro *et al.* (9) detected no Ca^{2+} currents (using up to 80 mM extracellular Ca^{2+}) through the *wv*GIRK2 channel expressed in Chinese hamster ovary cells. It has been suggested that Ca^{2+} influx through L-type Ca^{2+} channels contributes to the *weaver* phenotype (29). Our results show that Ca^{2+} may

indeed be considered as one contributing factor and that Ca^{2+} can enter directly through the *weaver* channel itself, perhaps followed later by entry through depolarization-activated Ca^{2+} channels. In a recent study, oocytes expressing *wv*GIRK2 died more quickly in solutions containing extracellular Ca^{2+} (10).

GIRK4 is the closest known homolog to GIRK2 (30) and has functional similarities that include the ability to form a GIRK channel in a complex with GIRK1 (31). We now find that these similarities extend to the effects of the *weaver* GYG-to-SYG mutation. *wv*GIRK4 channels bearing this mutation have functional characteristics similar to *wv*GIRK2 channels: constitutive activation (Fig. 3*C*), permeability to Na^+ as well as K^+ (Fig. 3), blockade by QX-314 and MK-801 (Fig. 3*A*), and permeability to Ca^{2+} (Fig. 2*B*). The observation that *wv*-GIRK1 is minimally functional by itself is consistent with suggestions that wild-type GIRK1 is always expressed in the context of a heteromultimer (21, 31, 32).

Because the GYG-to-SYG mutation also confers Na^+ conductance on the voltage-gated *shaker* K^+ channel (33), these data extend the present concept that this sequence plays a key role in determining the K^+ selectivity of K^+ channels in general. The regenerative pathophysiology suggested by our data gives a glimpse at the selective pressures that have led to conservation of the pore-region GYG sequence in many different K^+ channels.

We thank N. Dascal for comments. This work was supported by grants from the National Institute of Mental Health (MH-49176), the National Institute of General Medical Sciences (GM-29836), and the National Institute of Neurological Disorders and Stroke (NS-34407). P.K. held fellowships from the Guenther Foundation and the American Heart Association.

1. Patil, N., Cox, D. R., Bhat, D., Faham, M., Myers, R. M. & Peterson, A. S. (1995) *Nat. Genet.* **11,** 126–129.
2. Rakic, P. & Sidman, R. L. (1973) *Proc. Natl. Acad. Sci. USA* **70,** 240–244.
3. Willinger, M. & Margolis, D. M. (1985) *Dev. Biol.* **107,** 156–172.
4. Hatten, M. E., Liem, R. K. H. & Mason, C. A. (1986) *J. Neurosci.* **6,** 2676–2683.
5. Roffler-Tarlov, S. & Graybiel, A. M. (1986) *J. Neurosci.* **6,** 3319–3330.
6. Sekiguchi, M., Nowakowski, R. S., Nagato, Y., Tanaka, O., Guo, H., Madoka, M. & Abe, H. (1995) *Brain Res.* **696,** 262–267.
7. Slesinger, P. A., Patil, N., Liso, Y. J., Jan, Y. N., Jan, L. Y. & Cox, D. R. (1996) *Neuron* **16,** 321–331.
8. Kofuji, P., Hofer, M., Millen, K. J., James, H., Millonig, J. M., Davidson, N., Lester, H. A. & Hatten, M. E. (1996) *Neuron* **16,** 941–952.
9. Navarro, B., Kennedy, M. E., Velimirovic, B., Bhat, D., Peterson, A. S. & Clapham, D. E. (1996) *Science* **272,** 1950–1953.
10. Tucker, S. J., Pessia, M., Moorhouse, A. J., Gribble, F., Ashcroft, F. M., Maylie, J. & Adelman, J. P. (1996) *FEBS Lett.* **390,** 253–257.
11. Surmeier, D., Mermelstein, P. G. & Goldowitz, D. (1996) *Proc. Natl. Acad. Sci. USA* **93,** 11191–11195.
12. Mjaatvedt, A. E., Cabin, D. E., Cole, S. E., Long, L. J., Breitwieser, G. E. & Reeves, R. H. (1995) *Genome Res.* **5,** 453–463.
13. Lesage, F., Guillemare, E., Fink, M., Duprat, F., Heurteaux, C., Fosset, M., Romey, G., Barhanin, J. & Lazdunski, M. (1995) *J. Biol. Chem.* **270,** 28660–28667.
14. Sui, J. L., Chan, K. W. & Logothetis, D. E. (1996) *J. Gen. Physiol.* **108,** 381–392.
15. Choi, D. W. (1994) *Ann. N.Y. Acad. Sci.* **747,** 162–171.
16. Kofuji, P., Davidson, N. & Lester, H. A. (1995) *Proc. Natl. Acad. Sci. USA* **92,** 6542–6546.
17. Ashford, M. L. J., Bond, C. T., Blair, T. A. & Adelman, J. P. (1994) *Nature (London)* **370,** 456–459.
18. Peralta, E. G., Winslow, H. W., Peterson, G. L., Smith, D. H., Ashkenazi, A., Ramachandran, J., Schimerlik, M. I. & Capon, D. J. (1987) *Science* **236,** 600–605.
19. Wei, A., Solaro, C., Lingle, C. & Salkoff, L. (1994) *Neuron* **13,** 671–681.
20. Quick, M. W. & Lester, H. A. (1994) in *Ion Channels of Excitable Cells*, ed. Narahashi, T. (Academic, San Diego), pp. 261–279.
21. Hedin, K. E., Lim, N. F. & Clapham, D. E. (1996) *Neuron* **16,** 423–429.
22. Dascal, N. (1987) *CRC Crit. Rev. Biochem.* **22,** 317–387.
23. Boton, R., Dascal, N., Gillo, B. & Lass, Y. (1989) *J. Physiol. (London)* **408,** 511–534.
24. Hartzell, H. C. (1996) *J. Gen. Physiol.* **108,** 157–176.
25. Miledi, R. (1982) *Proc. R. Soc. London Ser. B* **215,** 491–497.
26. Barish, M. E. (1983) *J. Physiol. (London)* **342,** 309–325.
27. Silverman, S. K., Lester, H. A. & Dougherty, D. A. (1996) *J. Biol. Chem.* **271,** 30524–30528.
28. Kobayashi, T., Kazutaka, I., Ichikawa, T., Abe, S., Togashi, S. & Kumanishi, T. (1995) *Biochem. Biophys. Res. Commun.* **208,** 1166–1173.
29. Liesi, P. & Wright, J. M. (1996) *J. Cell Biol.* **134,** 477–486.
30. Lesage, F., Duprat, F., Fink, M., Guillemare, E., Coppola, T., Lazdunski, M. & Hugnot, J.-P. (1994) *FEBS Lett.* **353,** 37–42.
31. Krapivinsky, G., Gordon, E. A., Wickman, K., Velimirovic, B., Krapivinsky, L. & Clapham, D. E. (1995) *Nature (London)* **374,** 135–141.
32. Duprat, F., Lesage, F., Guillemare, E., Fink, M., Hugnot, J. P., Bigay, J., Lazdunski, M., Romey, G. & Barhanin, J. (1995) *Biochem. Biophys. Res. Commun.* **212,** 657–663.
33. Heginbotham, L., Lu, Z., Abramson, T. & MacKinnon, R. (1994) *Biophys. J.* **66,** 1061–1067.